JOURNAL OF CHEMICAL EDUCATION

Laboratory Experiment

pubs.acs.org/jchemeduc

Characterizing Crystalline-Vitreous Structures: From Atomically Resolved Silica to Macroscopic Bubble Rafts

Kristen M. Burson, Philomena Schlexer, Christin Büchner, Leonid Lichtenstein, Markus Heyde,* and Hans-Joachim Freund

Fritz-Haber-Institut der Max-Planck-Gesellschaft, Faradayweg 4-6, 14195 Berlin, Germany

Supporting Information

ABSTRACT: A two-part experiment using bubble rafts to analyze amorphous structures is presented. In the first part, the distinctions between crystalline and vitreous structures are examined. In the second part, the interface between crystalline and amorphous regions is considered. Bubble rafts are easy to produce and provide excellent analogy to recent research results on the atomic structure of silica glass. Ring statistics are employed to characterize the 2D structures and results from student bubble raft data are compared to results from atomically resolved images of amorphous 2D silica; the bubble rafts demonstrate good qualitative agreement. In these experiments, students learn how to characterize crystalline and amorphous materials and are introduced to current research results and analysis techniques for amorphous material structures.

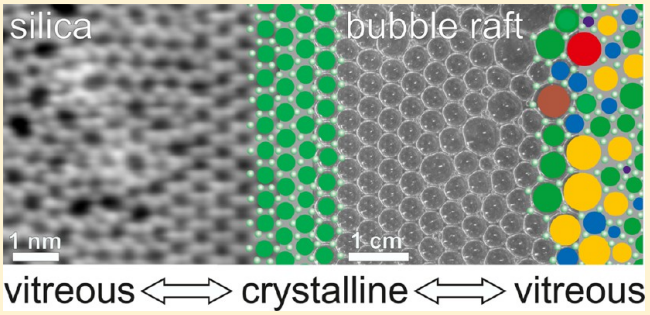

KEYWORDS: *Upper-Division Undergraduate, Surface Science, Crystals/Crystallography, Hands-On Learning/Manipulative, Laboratory Instruction, Materials Science*

MOTIVATION

Material structure is a canonical element within undergraduate chemistry instruction. Understanding the structural arrangement on the atomic level is essential for understanding and predicting materials' properties from the microscopic to the macroscopic level.[1] For crystalline materials, the atomic structure can often be recognized by the macroscopic shape; daily examples are table salt, sugar, diamonds, and snowflakes. Metals often form hexagonal close-packed or face-centered cubic structures. In these cases, Miller indices and basis vectors offer a quantitative description of structure. Amorphous materials, in contrast, evade a similarly concise structural description due to the lack of long-range order. Common examples for amorphous materials are glasses, wax, and plastics. Silicon dioxide is the most prominent glass network former. This materials class finds its applications in windows and smart phones, but also as a gate dielectric for transistors and as oxide supports for catalysis.[2] Amorphous structures are also readily observed on the macroscale. The soapy foam when showering, the head on cold beer, and the frothy whitecaps of breaking ocean waves are more disordered than crystalline in nature. Given the prevalence of amorphous systems, it seems prudent to incorporate educational exercises which address them.

Here, we present a set of laboratory explorations in which students develop structural descriptions of amorphous materials by using a bubble raft to highlight the similarities between macroscopic and microscopic amorphous systems. Recently, images of the atomic structure of amorphous glass have been obtained by scanning probe microscopy (SPM) and verified by transmission electron microscopy (TEM).[3−6] SPM and TEM are surface science techniques which can yield atomic resolution in real space and are widely used in the fields of physics, chemistry, and biology. Several examples of their use within an educational context have been reported and could be used prior to the laboratory exercises presented here, with an emphasis on determination of material structure.[7,8] Bubble rafts provide a hands-on, visible analogy to the atomic structure of glass and are cost-effective to produce. Bubble rafts have been used since as early as 1947 to show crystalline structures and defects.[9−11] They provide a simplified two-dimensional (2D) model of complex three-dimensional (3D) structures. Because the bubble rafts exhibit many of the complexities observed in atomically resolved images of amorphous materials, these experiments move student thinking beyond overly simplistic structural models and introduce students to current research and analysis techniques. The experiments presented here were originally developed for an undergraduate in our laboratory as part of a longer term project. Due to the rich analysis possibilities for the bubble raft system, we have adapted the project for use as a single or multi session laboratory exercise. Here, we present two experiments utilizing the bubble raft model system in which students learn to describe the structure of amorphous materials both conceptually and using statistical methods. The first addresses the distinctions between

DOI: 10.1021/acs.jchemed.5b00056
J. Chem. Educ. XXXX, XXX, XXX−XXX

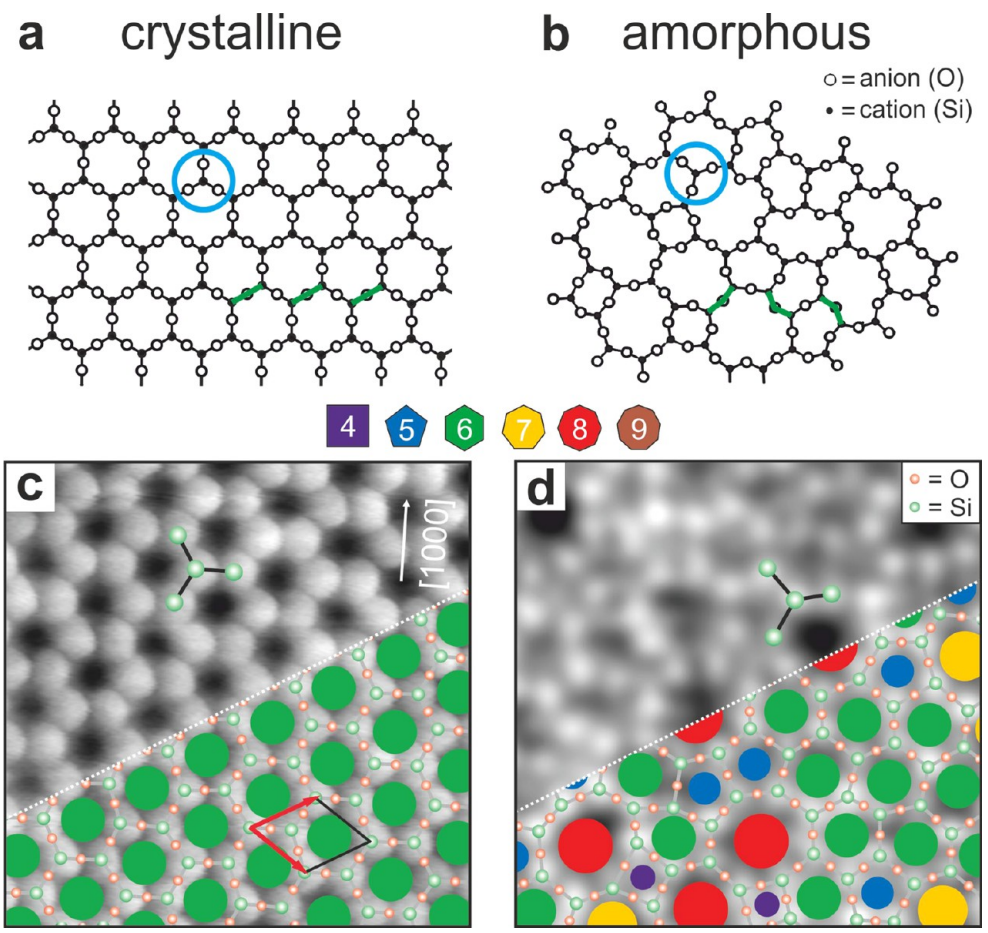

Figure 1. Model amorphous materials. Random network model by W. H. Zachariasen shown along with atomically resolved scanning tunneling microscopy images of silica for (a and c) crystalline and (b and d) amorphous regions.[14] Images c and d are 3.5 nm × 3.5 nm with the [1000] direction of the underlying Ru substrate indicated in (c). Both crystalline and amorphous structures exhibit the same building unit, marked with a blue circle in the model and with connected green circles in the experimental images, but different angles between these units (green lines in (a) and (b)). The crystalline unit cell is marked in (c) along with the basis vectors indicated by red arrows.

crystalline and amorphous systems and utilizes ring size statistics as a tool for characterizing amorphous systems. The second addresses the interface between crystalline and vitreous domains and asks students to define transition regions in these systems. Both experiments have clear analogy to the recent achievement of atomically resolved images of silica glass, which we discuss first to provide background and context.

BACKGROUND

The atomic structure of amorphous materials has long been a mystery. Zachariasen developed a model 80 years ago to predict the structure of crystalline and amorphous materials.[12] The model, referred to as random network theory, assumes that materials consist of a network of building blocks with the same chemical connectivity regardless of whether the material is crystalline or amorphous. For SiO_2, the building blocks are tetrahedral with an oxygen atom at each corner and a silicon atom in the center. Corner sharing tetrahedral building blocks can be assembled into either crystalline or vitreous configurations. To simplify the complicated 3D arrangements, Zachariasen used a 2D representation to describe amorphous materials, shown in Figure 1a,b. In the 2D representation of SiO_2, each silicon is connected to three oxygens, as shown by the blue circle in Figure 1a,b. Zachariasen's model was consistent with X-ray diffraction data of oxide materials, but at the time more definitive empirical verification of the model was lacking.[13]

For crystalline materials, diffraction methods with X-ray or neutron beams yield discrete patterns. These methods average over macroscopic sample areas and provide information in reciprocal space. While diffraction methods can provide information about average density for amorphous materials, they fail to provide a direct, real space view of the atomic arrangement and, as such, are not sufficient to describe atomic structure in amorphous systems.

The development of SPM and derivative techniques has significantly advanced fundamental understanding of material structure and related material properties.[15,16] These techniques can reveal real space atomic structure information that complements and enhances earlier investigations with traditional diffraction techniques. Yet even with SPM-based techniques, atomic resolution of complex surface structures remains a challenge.[17−22] Initial attempts to resolve the atomic structure of glassy materials failed to yield full atomic resolution, likely related to the complex interactions between the tip used for microscopy and the rough (not atomically flat) 3D nature of the structure.[23] Only recently, by developing a new class of 2D amorphous materials, have clear atomically resolved images been achieved. SiO_2 is a prototype for amorphous networks. A 2D silica bilayer has been successfully

DOI: 10.1021/acs.jchemed.5b00056
J. Chem. Educ. XXXX, XXX, XXX−XXX

produced which retains many of the structural and physical properties of its 3D analogue while simultaneously allowing for detailed characterization with scanning probe. Additionally, the silica bilayers can reproduce both amorphous and crystalline structures present in their bulk counterparts. Figure 1c,d shows a comparison between the atomic resolution scanning tunneling microscopy (STM) images of crystalline and vitreous bilayer silica. The structures show a striking similarity to Zachariasen's early postulates.[5] On the basis of these images, quantitative descriptions of the vitreous material have been established using ring size statistics.

Such quantitative descriptions of 2D amorphous systems are not limited to bilayer silica. In a recent publication, ring statistics were also used to characterize defect-rich $CuO_2(111)$, an amorphous polymer network, and even macroscopic bubble rafts.[24] Despite different size scales, these diverse systems show some similar characteristics. In the following section, we discuss how the bubble rafts can be used as a tangible example of amorphous systems and present two laboratory exercises to quantitatively characterize the amorphous system.

PROCEDURE

A bubble raft is a simple physical model consisting of a planar array of soap bubbles.[9] Bubble rafts provide a 2D model for crystalline materials, simulating grain boundaries and zero-dimensional defects. They have been used previously for teaching purposes.[25−28] They have also been used to investigate the behavior of a bulk material under mechanical strain.[11,29−31] For example, in 1947, L. Bragg and J. F. Nye used bubble rafts as 2D models to illustrate intercrystalline boundaries and plastic flow in metals.[10] Bubble rafts can be used to simulate amorphous structures as well.[32]

In this study, both crystalline and amorphous bubble rafts were produced and their topological characteristics analyzed. We produced the bubbles in a shallow 4 in. diameter Petri dish in a solution of 0.4 mass % glycerin, 0.3 mass % dish soap, and 99.3 mass % water using a syringe-needle with a flat end, as shown in Figure 2a. The needle had a diameter of 0.6−0.8 mm and was connected to the exhaust of a membrane pump with adjustable air pressure. For crystalline bubble rafts, the needle was dipped in the solution and an optimal flow rate was determined by adjusting the air pressure. The needle was then moved back and forth at a constant speed and penetration depth. To create the amorphous network, slight variations in the lateral needle movement and penetration depth were induced randomly to produce bubbles with different sizes.[11] A combination of these two techniques was used to create crystalline−vitreous interfaces. A standard digital camera was used to take images of the bubble rafts for further analysis. Constant imaging mode was used due to the short bubble lifetime (∼1 min). In principle, these networks can also be attained by carefully blowing bubbles through tubing connected to a needle and documenting the resulting rafts with a smart phone camera. We found that needles with a flat-ended opening produced better bubbles than needles with an angled end.

Once data is collected, both the crystalline and amorphous structures are analyzed. The space between three neighboring bubbles was defined as the connection point in order to develop ring statistics, indicated by green circles for both crystalline and vitreous bubble rafts in Figure 2b,c. Like the silica system, there is trigonal connectivity in the bubble raft, as indicated by the black connection lines in Figure 2c. The

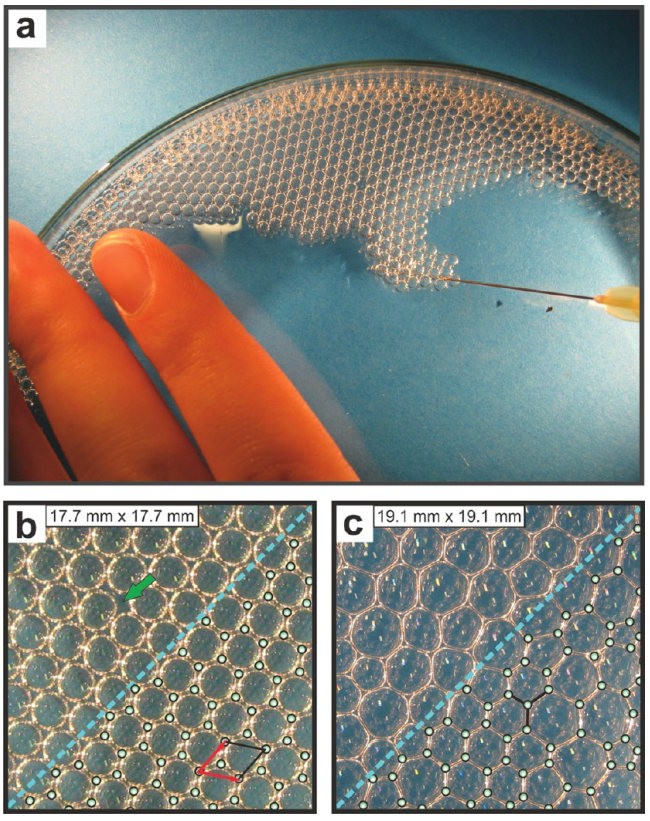

Figure 2. Bubble raft preparation. (a) Bubble raft creation technique with glycerin solution and flat ended syringe needle. Crystalline (b) and amorphous (c) bubble rafts are produced. Images b and c are 17.7 mm × 17.7 mm. Connection points are indicated in green and the trigonal connectivity is displayed with black connection lines in (c). For the crystalline raft, a unit cell (black) and basis vectors (red) are shown. A 0-dimensional defect (green arrow) can also be seen.

connection points surrounding a given bubble define a polygon shape. Because atomic structures exhibit rings of bonded atoms, we refer to this polygon as an *n*-membered ring, where *n* is the number of connection points. We used this description to compare the ring size statistics for amorphous and crystalline structures (Figure 2b,c). A more detailed description of the experimental setup, analysis, and possible modifications is provided in the Supporting Information.

HAZARDS

There are no major hazards associated with the lab. Ingestion of the solution should be avoided and care should be taken in handling sharp needles.

EXPERIMENTS

Experiment 1: Crystalline and Vitreous Structures

Figure 2b shows a crystalline bubble raft. The bubbles in this raft are 6-membered rings and exhibit a similar size and shape. There is also one defect present in the structure, indicated by the green arrow. As with atomic descriptions of crystals, the crystalline bubble rafts can be described by a set of basis vectors and students can determine the characteristic length scales which define the lattice. Figure 2b displays the unit cell with a two atom-basis, outlined in black, as well as two basis vectors in red. The key question, though, comes in comparing crystalline bubble rafts with amorphous bubble rafts: How are amorphous

DOI: 10.1021/acs.jchemed.5b00056
J. Chem. Educ. XXXX, XXX, XXX−XXX

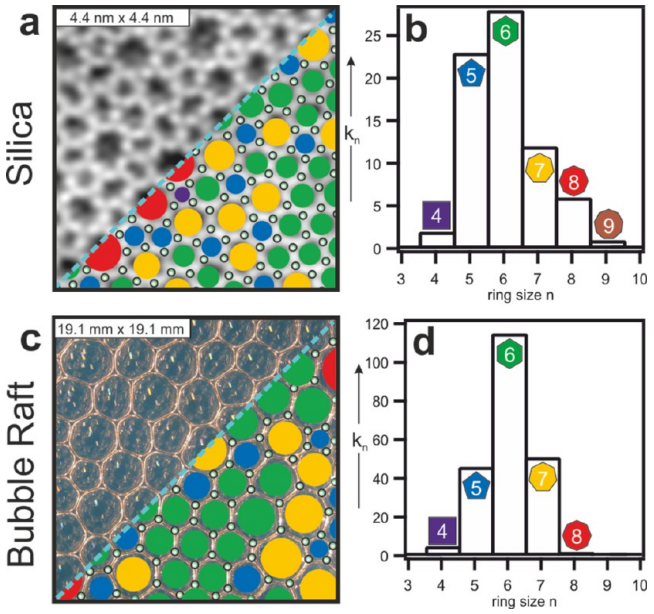

Figure 3. Ring statistics. Amorphous silica (a) and an amorphous bubble raft (c). Connection points are indicated with green circles and ring sizes are color coded. Histograms show the number of rings with each ring size (k_n) for the amorphous silica (b) and the bubble raft (d).

materials different from crystalline materials and how can these amorphous systems be characterized? In Figure 3, panels a and c show an image of a STM image of amorphous bilayer silica and an amorphous bubble raft, respectively. Unlike in the crystalline system, there is no evidence of long-range order and the rings exhibit nonuniform sizes, shapes, and orientations. Thus, for these systems, students can be introduced to statistical tools for characterizing nonideal or noncrystalline systems. For this study, we employed ring size distributions to describe the systems. Panels b and d of Figure 3 show the ring size distributions for the amorphous silica bilayer and the bubble raft, respectively. In both systems, six-membered rings are the most prevalent, followed by five- and seven-membered rings. Four-, eight-, and nine-membered rings were less common.

The ring statistics provide a quantitative description of the amorphous structure and allow one to compare and contrast different amorphous systems.[24] For example, while the amorphous silicon and the bubble raft exhibit similar qualitative behavior, the silica ring distribution shows a greater asymmetry in reference to a normal distribution. Five-membered rings are more common than seven-membered rings, and eight-membered rings are more common than four-membered rings. The statistics agree well with the log-normal distribution of the ring size used previously by Shackelford to describe ideal 2D triangular networks.[24,33] In contrast, the bubble raft system exhibits nearly equal probabilities for five- and seven-membered rings. While the ring distributions for the bubble raft and the silica are not identical, they are both governed by the geometric constraints imposed by the two-dimensionality of the systems. For a closed 2D planar structure, Euler's theorem predicts the following constraint for the population of different ring sizes:

$$\sum (6 - n)k_n = 0$$

Here, k_n is the number of rings having n sides.[34] The value of 0 is achieved when curvature induced by rings smaller than 6 is compensated by rings larger than 6, contributing inverse curvature of the same absolute value. A sum which deviates from 0 indicates a deformation of the flat 2D structure. A sphere, for example, will have a sum of 12 (a C_{60} fullerene, comparable to a soccer-ball structure, has 12 five-membered rings and 20 six-membered rings yielding a sum of 12). For the bubble raft, the sum yields a value of 1, and for the silica film system, the sum is 0. The ring statistics are thus consistent with expectations based on 2D geometric constraints. In the lab, students analyze ring statistics of amorphous bubble rafts and compare their results with Euler's formula. Students were able to identify differences in the ring size distributions between silica and the bubble rafts and were also able to establish agreement with Euler's equation for the bubble rafts. As a supplementary exercise, these geometric constraints can also be experienced in building structures from a chemical model kit. Students will find that for a flat structure larger ring sizes must be balanced with smaller ring sizes. For example, two five-membered rings will alleviate the strain introduced by an eight-membered ring. It should also be noted that there is a larger "bond length" variation in the bubble raft than in the silica. Therefore, bubble rafts do not precisely reproduce the features of the silica system quantitatively but rather provide a comprehensive qualitative model for atomic level amorphous structure.

Experiment 2: Crystalline–Vitreous Interfaces

The glass transition process is not fully understood, but there is great interest in understanding how liquid solidifies into an amorphous or crystalline state. Crystalline–vitreous interfaces provide clues about the physical mechanisms that govern these dynamic processes. Many studies have been conducted concerning crystalline–amorphous interfaces.[35] One example of a technologically important interface is that of crystalline silicon and amorphous silicon dioxide, which appears ubiquitously in the semiconductor industry. Looking at these systems, one may seek to identify whether there is a discrete boundary or a continuous transition at the crystalline–vitreous interface and to quantify its location and spatial extent. Ring statistics, introduced above, provide one metric for characterizing the boundary. Figure 4 shows a comparison of the crystalline–vitreous interface for silica and bubble rafts. It can be observed that the transitions maintain trigonal connectivity and do not exhibit large holes; they are continuous. To quantify the crystalline–vitreous transition, the images were divided into 11 segments of equivalent width (Figure 4e,f) and the number of n-membered rings in each segment was counted (as described in ref 3). As shown in Figure 4g,h, at the interface from crystalline to vitreous, five- and seven-membered rings are introduced first, while four-, eight-, and nine-membered rings display greater prevalence later in the amorphous phase. To further quantify the transition, we consider the crystallinity as a function of lateral position. Here, we define crystallinity as

$$C(x) = \frac{k_6(x)}{\sum_{n=4}^{9} k_n(x)}$$

where $k_n(x)$ represents the number of n-membered rings within a slice at lateral position x.[4] Figure 4i,j show the crystallinity as a function of lateral coordinate for both the silica and the bubble raft. In both cases, the quantitative calculation of the crystallinity indicates that the spatial transition in the degree of crystallinity is continuous. Here, the crystalline–vitreous interface is best described with a transition region width rather

DOI: 10.1021/acs.jchemed.5b00056
J. Chem. Educ. XXXX, XXX, XXX–XXX

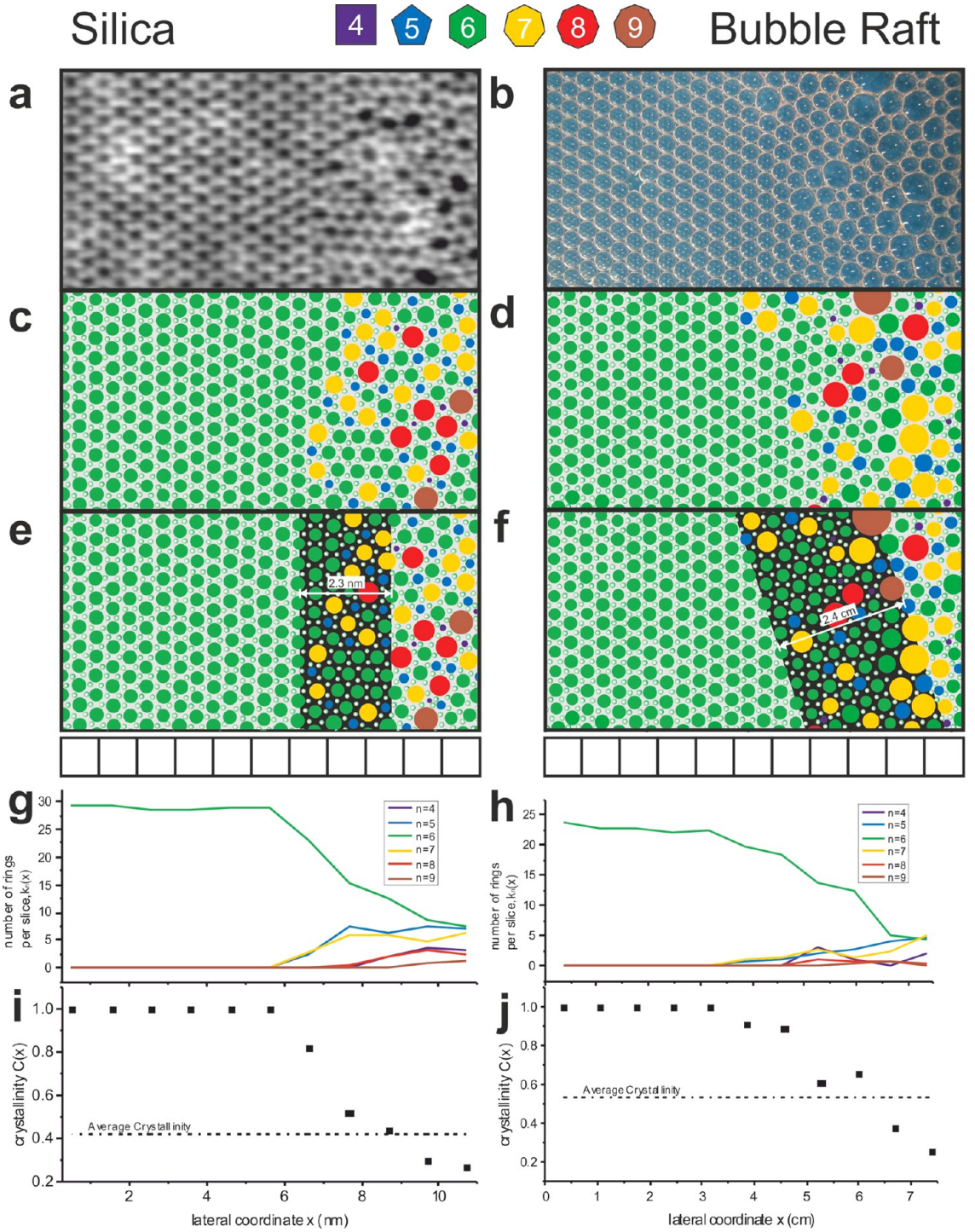

Figure 4. Crystalline−amorphous interface. The crystalline−amorphous (left−right) interface is shown for (a) an STM image of silica and for the (b) bubble raft. (c and d) Color-coded ring characterization for the images a and b displaying the introduction of non-six-membered rings in the transition from the crystalline region to the amorphous region. (e and f) Region through which the continuous transition between crystalline and vitreous occurs; images are divided into 11 equivalent segments for image analysis, as shown below the figures. (g and h) Quantitative analysis of the population of distinct ring sizes with respect to lateral position shows a continuous transition from crystalline to vitreous domains. (i and j) Crystallinity as a function of lateral position.

than a single discrete domain boundary. The vitreous average crystallinity can be used as a metric for the "end" of the transition region. On the basis of the ring statistics determined above, the vitreous bubble raft has an average crystallinity of 0.53. The interface width for the bubble raft shown is approximately 2.4 cm, indicated by the shaded region in Figure 4f. The crystalline lattice of the bubble raft image was aligned with the lattice direction of the silica bilayer. Next, to more accurately reflect the true transition width, a transformation was applied to account for the angle of the interface with respect to the crystal lattice direction (described in Supporting Information). Here, the edges of the transition region are represented as straight lines for consistency with the analysis approach, but it should be noted that a more winding interface

DOI: 10.1021/acs.jchemed.5b00056
J. Chem. Educ. XXXX, XXX, XXX−XXX

is evident in larger scale images. To compare the width of the bubble raft transition to other systems, we define a "normalized distance unit" as the average distance between two adjacent connection points in the crystalline phase. In this case, the transition width corresponds to approximately 13 normalized distance units (0.18 cm). In contrast, the thickness of the transition region for the silica shown in Figure 4g is approximately 2.3 nm, corresponding to approximately 8 normalized distance units. Given the similar transition region trends exhibited by the two systems, bubble rafts provide a good analogy to the atomic system and therefore are an instructive model to reproduce and analyze transition characteristics.

CONCLUSIONS

In a self-assessment of learning from the lab, one student commented that they learned "what amorphous and crystalline structures are and how one can differentiate them with mathematical calculations." Overall, we noticed that student lab reports indicated a more detailed understanding of amorphous systems than attained from their previous coursework. Bubble rafts provide a tangible exploration ground for students to investigate the question of what defines crystalline and vitreous systems. They provide qualitative analogy to the atomic structure of vitreous and crystalline systems and, as such, allow students to delve into analysis techniques for these systems. Here, we have proposed two projects for students to examine the differences between crystalline and vitreous systems and the vitreous and crystalline interface.

ASSOCIATED CONTENT

Supporting Information

Instructor notes, student handouts, sample data, and analysis details are provided. This material is available via the Internet at http://pubs.acs.org.

AUTHOR INFORMATION

Corresponding Author

*E-mail: heyde@fhi-berlin.mpg.de.

Notes

The authors declare no competing financial interest.

ACKNOWLEDGMENTS

We wish to thank Thomas Ebbesen for helpful discussion. We also wish to thank the students of 2. FS Master Sommersemester 2015 of the Humboldt University for useful feedback on the laboratory instructional materials.

REFERENCES

(1) Galasso, F. The Importance of Understanding Structure. *J. Chem. Educ.* **1993**, *70*, 287.
(2) Zallen, R. *The Physics of Amorphous Solids*; Wiley-VCH: New York, 1998.
(3) Lichtenstein, L.; Büchner, C.; Yang, B.; Shaikhutdinov, S.; Heyde, M.; Sierka, M.; Włodarczyk, R.; Sauer, J.; Freund, H.-J. The Atomic Structure of a Metal-Supported Vitreous Thin Silica Film. *Angew. Chem., Int. Ed.* **2012**, *51*, 404−407.
(4) Lichtenstein, L.; Heyde, M.; Freund, H.-J. Crystalline-Vitreous Interface in Two Dimensional Silica. *Phys. Rev. Lett.* **2012**, *109*, 106101.
(5) Lichtenstein, L.; Heyde, M.; Freund, H.-J. Adsorption of Au and Pd on Ruthenium-Supported Bilayer Silica. *J. Phys. Chem. C* **2012**, *116*, 20426−20432.
(6) Huang, P. Y.; Kurasch, S.; Alden, J. S.; Shekhawat, A.; Alemi, A. A.; McEuen, P. L.; Sethna, J. P.; Kaiser, U.; Muller, D. A. Imaging Atomic Rearrangements in Two-Dimensional Silica Glass: Watching Silica's Dance. *Science* **2013**, *342*, 224−227.
(7) Hipps, K. W.; Scudiero, L. Electron Tunneling, a Quantum Probe for the Quantum World of Nanotechnology. *J. Chem. Educ.* **2005**, *82* (5), 704.
(8) Heinz, W. F.; Hoh, J. H. Getting Physical with Your Chemistry: Mechanically Investigating Local Structure and Properties of Surfaces with the Atomic Force Microscope. *J. Chem. Educ.* **2005**, *82* (5), 695.
(9) Bragg, L. S.; Nye, J. F. Ein Dynamisches Modell Einer Kristallstruktur. *Naturwissenschaften* **1947**, *34*, 328−336.
(10) Bragg, L.; Lomer, W. M. A Dynamical Model of a Crystal Structure. *Proc. R. Soc. London, Ser. A* **1949**, *196*, 171−181.
(11) Arciniaga, M.; Kuo, C.-C.; Dennin, M. Size Dependent Brittle to Ductile Transition in Bubble Rafts. *Colloids Surf., A* **2011**, *382*, 36−41.
(12) Zachariasen, W. H. The Atomic Arrangement in Glass. *J. Am. Chem. Soc.* **1932**, *54*, 3841−3851.
(13) Warren, B. E. X-ray Determination of the Structure of Glass. *J. Am. Ceram. Soc.* **1934**, *17*, 249−254.
(14) Lichtenstein, L.; Heyde, M.; Freund, H.-J. Atomic Arrangement in Two-Dimensional Silica: From Crystalline to Vitreous Structures. *J. Phys. Chem. C* **2012**, *116*, 20426−20432.
(15) Binnig, G.; Quate, C. F.; Gerber, C. Atomic Force Microscope. *Phys. Rev. Lett.* **1986**, *56*, 930−933.
(16) Binnig, G.; Rohrer, H.; Gerber, C.; Weibel, E. Surface Studies by Scanning Tunneling Microscopy. *Phys. Rev. Lett.* **1982**, *49*, 57−61.
(17) Raberg, W.; Wandelt, K. Atomically Resolved AFM Investigations of an Amorphous Barium Silicate Surface. *Appl. Phys. A: Mater. Sci. Process.* **1998**, *66*, 1143−1146.
(18) Burgler, D. E.; Schmidt, C. M.; Schaller, D. M.; Meisinger, F.; Schaub, T. M.; Baratoff, A.; Guntherodt, H. J. Atomic-Scale Scanning Tunneling Microscopy of Amorphous Surfaces. *Phys. Rev. B* **1999**, *59*, 10895−10902.
(19) Schlenz, H.; Kirfel, A.; Schulmeister, K.; Wartner, N.; Mader, W.; Raberg, W.; Wandelt, K.; Oligschleger, C.; Bender, S.; Franke, R.; Hormes, J.; Hoffbauer, W.; Lansmann, V.; Jansen, M.; Zotov, N.; Marian, C.; Putz, H.; Neuefeind, J. Structure Analyses of Ba-Silicate Glasses. *J. Non-Cryst. Solids* **2002**, *297*, 37−54.
(20) Poggemann, J.-F.; Heide, G.; Frischat, G. H. Direct View of the Structure of Different Glass Fracture Surfaces by Atomic Force Microscopy. *J. Non-Cryst. Solids* **2003**, *326−327*, 15−20.
(21) Frischat, G. H.; Poggemann, J.-F.; Heide, G. Nanostructure and Atomic Structure of Glass Seen by Atomic Force Microscopy. *J. Non-Cryst. Solids* **2004**, *345−346*, 197−202.
(22) Raberg, W.; Ostadrahimi, A. H.; Kayser, T.; Wandelt, K. Atomic Scale Imaging of Amorphous Silicate Glass Surfaces by Scanning Force Microscopy. *J. Non-Cryst. Solids* **2005**, *351*, 1089−1096.
(23) Burson, K. M.; Yamamoto, M.; Cullen, W. G. Modeling Noncontact Atomic Force Microscopy Resolution on Corrugated Surfaces. *Beilstein J. Nanotechnol.* **2012**, *3*, 230−237.
(24) Buechner, C.; Schlexer, P.; Lichtenstein, L.; Stuckenholz, S.; Heyde, M.; Freund, H.-J. Topological Investigation of Two-Dimensional Amorphous Materials. *Z. Phys. Chem.* **2014**, *228*, 587−607.
(25) Bragg, L.; Nye, J. F. A Dynamical Model of a Crystal Structure. *Proc. R. Soc. London, Ser. A* **1947**, *190*, 474−481.
(26) McCormick, P. D. Solid State Labs: The Bubble Raft. *J. Chem. Educ.* **1975**, *52*, 521.
(27) Dungey, K. E.; George Lisensky, S. Michael Condren. Kixium Monolayers: A Simple Alternative to the Bubble Raft Model for Close-Packed Spheres. *J. Chem. Educ.* **2000**, *77*, 618.
(28) Geselbracht, M. J.; Ellis, A. B.; Penn, R. L.; Lisensky, G. C.; Stone, D. S. Mechanical Properties of Metals: Experiments with Steel, Copper, Tin, Zinc, and Soap Bubbles. *J. Chem. Educ.* **1994**, *71*, 254.

DOI: 10.1021/acs.jchemed.5b00056
J. Chem. Educ. XXXX, XXX, XXX−XXX

(29) Argon, A. S.; Kuo, H. Y. Plastic-Flow in a Disordered Bubble Raft (an Analog of a Metallic Glass). *Mater. Sci. Eng.* **1979**, *39*, 101−109.
(30) Georges, J. M.; Meille, G.; Loubet, J. L.; Tolen, A. M. Bubble Raft Model for Indentation with Adhesion. *Nature* **1986**, *320*, 342−344.
(31) Bragg, L. A Model Illustrating Intercrystalline Boundaries and Plastic Flow in Metals. *J. Sci. Instrum.* **1942**, *19*, 148−150.
(32) Simpson, A. W.; Hodkinson, P. H. Bubble Raft Model for an Amorphous Alloy. *Nature* **1972**, *237*, 320−322.
(33) Shackelford, J. F. A Gas Probe Analysis of Structure in Bulk and Surface-Layers of Vitreous Silica. *J. Non-Cryst. Solids* **1982**, *49*, 19−28.
(34) Ebbesen, T. W. Cones and Tubes: Geometry in the Chemistry of Carbon. *Acc. Chem. Res.* **1998**, *31*, 558−566.
(35) Wooten, F.; Weaire, D. A Computer-Generated Model of the Crystalline Amorphous Interface in Silicon. *J. Non-Cryst. Solids* **1989**, *114* (Part 2), 681−683.

DOI: 10.1021/acs.jchemed.5b00056
J. Chem. Educ. XXXX, XXX, XXX−XXX